

Interaction of 3-Hydroxypicolinamide with Tb^{III} and its Sensitizing Effect on Terbium Luminescence as a Function of pH and Medium

Thangjam Promila Devi^{a,b}, Phanjoubam Pengkiliya^a and Lonibala Rajkumari^{a,*}

^aDepartment of Chemistry, Manipur University, Canchipur 795 003, Imphal, Manipur, India.

^bDepartment of Chemistry, Liberal College, Luwangshangbam, Koirengi, Imphal, Manipur, India.

Received 4 October 2014, revised 12 November 2014, accepted 19 November 2014.

ABSTRACT

Coordination behaviour of 3-hydroxypicolinamide (HPA) towards Tb^{III} is studied in aqueous and micellar media. The complex formed exists as ML₂ species in which HPA behaves as an O,O,N,N-chelating ligand. The solid complex is isolated from aqueous medium and characterized employing elemental analysis, TG/DTA, magnetic, IR, ESR and mass spectral data. Stability constant and other accompanying thermodynamic parameters of the Tb(III) complex have been determined pHmetrically. The complexation reaction is spontaneous and exothermic. Effect of micelles and pH on the luminescence of Tb(III) were also studied. The emission peaks of Tb^{III} are highly sensitized on complexation with HPA and the optimum luminescence efficiency is obtained in slightly acidic to neutral solutions (pH 6–8). The complex decays biexponentially and the presence of ethanol and surfactants causes a large increase in the luminescence intensity protecting the complex from radiationless deactivation processes.

KEYWORDS

3-Hydroxypicolinamide, stability constant, micelles, terbium luminescence, sensitization.

1. Introduction

In recent years, the emission from lanthanide ions has been utilized extensively in biological systems. The applications range from luminescent labels of biologically-relevant molecules as components of bioassays,^{1–7} spatially localized sensors and contrast agents,^{8–15} as donors in time-resolved energy transfer systems,^{16–18} to the detection of cellular functions *in vivo* to the elucidation of structure and function of enzymes and proteins^{19–21} and use as diagnostic tools.^{22–25}

Amongst the lanthanides, the most important role in biochemical studies falls on Eu^{III} and Tb^{III} ions, due to the fact that their resonance energy levels overlap the triplet energy states of protein and nucleic acid aromatic residues leading to enhancement of their natural fluorescence by energy transfer when irradiated with ultraviolet light.^{1,26,27} Sensitization of luminescence which is common in Tb(III) complexes results from the energy transfer from the lowest-lying ligand triplet excited state to the emissive ⁵D₄ state of the metal ion. For strong chelators, the energy of the donor triplet state which must lie above the ⁵D₄ excited state of Tb^{III} is the most important parameter for efficient energy transfer to take place. Since Ln^{III} possess many similarities in their properties to Ca^{II}, the isomorphous replacement of Ca^{II} by Ln^{III} holds the promise of exploiting the rich and various spectroscopic properties of Ln^{III} for obtaining information on the structure of Ca^{II} in biological systems.^{22,28–32} Their ability to substitute Zn^{II} and Mg^{II} at their binding sites also makes lanthanide luminescence a useful tool to study biomolecules complexed to Zn^{II} and Mg^{II} ions.²²

Although trivalent lanthanide ions have weak absorption coefficients, highly luminescent lanthanide complexes have been prepared by chelating strongly absorbing organic ligands to the lanthanide ions.³³ In such cases, a synergistic effect often

referred to as an ‘antenna-effect’ occurs between the ligand and the lanthanide ion, where the absorbed energy by the ligand is transferred intramolecularly from the ligand triplet state to the lower lying emissive lanthanide excited state. The possibility of having ligands that function as light-harvesting units in lanthanide complexes has been investigated.³³ Amongst the ligands that serve as light-absorbing antennas, we are interested in the coordination modes and photoluminescence behaviour of the lanthanide complexes of pyridine carboxylic acids. Dipicolinic acid (DPA) and its derivatives have been shown to greatly enhance Tb^{III} emission upon complexation owing to favourable energy transfer from the ligand’s 3pp* excited state to the ⁵D₄ excited state of the metal ion. The energy transfer mechanisms between the lanthanide ions and other pyridine carboxylic acid ligands based on the luminescence of the lanthanide(III) complexes have been reported.^{34–44} 3-Hydroxypicolinamide (HPA, Fig. 1) used in the present work is a potential ligand with different chelating modes^{45–48} including O,N,O-chelation (as monoprotonated tridentate ligand through deprotonated phenolate oxygen, the pyridine nitrogen and the amido carbonyl oxygen) or O,O-chelation (as monoprotonated bidentate ligand through deprotonated phenolate oxygen and the amido carbonyl oxygen) or O,N-chelation (as protonated species through the amido carbonyl oxygen and the pyridine nitrogen). This compound is fluorescent and generally used^{49,50} as a model compound for the study of chelating ability and fluorescence of the antibiotic Virginiamycin S (VS). HPA is reported⁴⁶

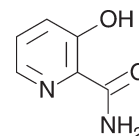


Figure 1 Structure of HPA.

*To whom correspondence should be addressed. E-mail: lonirk@yahoo.co.uk

to form a highly luminescent Zn(II) complex in which the hydroxy group at the 3-position of the pyridine ring plays a key role in achieving luminescence. We, therefore, aim to study the coordinating behaviour of HPA towards Tb^{III} and the luminescent properties of the complex. We are also interested to investigate the sensitizing effect, if any, of surfactants on terbium luminescence. Changes on terbium luminescence as a function of pH is also discussed and reported here.

2. Experimental

2.1. Materials and Methods

Terbium chloride monohydrate, 3-hydroxypicolinamide, the surfactants (triton-100, Tx-100 and (cetyltrimethylammonium-bromide, CTAB) were purchased from Sigma-Aldrich and used as received. All other chemicals used in this study are of AR grade.

C, H and N were microanalysed using a Perkin-Elmer 2400-II elemental analyzer while Tb content was estimated complexometrically.⁵¹ Thermal studies were carried out under N₂ atmosphere on a Perkin-Elmer STA 6000 simultaneous thermal analyzer in the temperature range 35–850 °C at a heating rate of 10 °C min⁻¹. A Sherwood magnetic susceptibility balance was used for the room temperature magnetic susceptibility measurement using CuSO₄·5H₂O as standard while IR spectra were recorded on a Shimadzu FTIR-8400S spectrometer in the range 4000–400 cm⁻¹ using KBr pellets. ESR spectra were obtained on a JEOL, JES-FA 200 ESR spectrometer (X-band) using tempol as field marker. Mass spectra were obtained using a Thermo Finigan LCQ Advantage max ion trap mass spectrometer.

Luminescence spectral measurements were performed with a Perkin-Elmer LS-55 fluorescence spectrometer equipped with 20 kW Xenon discharge lamp and the spectra were recorded in solution by mixing the required amount of ligand and metal salt in desired molar ratio in different media/pH. Tb(III) luminescence lifetimes were monitored around the most intense transition of the cation ($\lambda_{em} = 546$ nm). Potentiometric experiments for the complexation of Tb^{III} with HPA were carried out on a digital Eutech Cyberscan-5500 pH-meter at desired temperatures using a Haake DC-10 constant temperature bath. The experimental details for the above two techniques were explained elsewhere.⁵²

2.2. Preparation of the Solutions for the pHmetric Titration

All the solutions used in the pHmetric studies were prepared only in double-distilled water. 25 mL of three sets of solutions (a), (b) and (c) having the following compositions were prepared by making up the volume with double-distilled water.

Solution (a): [5 mL KNO₃ (0.1 mM) + 1.48 mL HNO₃ (0.1 M) + 3.75 mL ethanol],

Solution (b): [Solution (a) + 3.75 mL HPA (3 mM)] and

Solution (c): [Solution (b) + 0.15 mL TbCl₃ (0.6 mM)].

To each of the solution mixtures to be used for the pH-metric titrations in CTAB micellar media, 1.5 mL of 3 mM CTAB was added before making up the volume. The pHmetric titration of solutions (a), (b) and (c) was carried out with standard 0.05 M KOH solution at 0.1 M KNO₃ ionic strength at four different temperatures, 15, 25, 35 and 45 °C. In all the reaction mixtures, 1:3 metal:ligand molar ratio was maintained and all the titrations were carried out at the pH range 3.50–10.50.

2.3. Calculations

The complexation parameters have been calculated using the following equations given by Bjerrum⁵³ and modified by Irving

and Rossotti.⁵⁴ The average number of protons, \bar{n}_H , associated with HPA at various pH-meter readings were calculated from acid and ligand titration curves using equation (1):

$$\bar{n}_H = Y - \frac{(V_L - V_A)(N + E^0)}{(V_0 + V_A)T_L^0} \quad (1)$$

where Y is the number of dissociable protons present in the ligand. V_L and V_A are the volumes of KOH of concentration N (0.05 M) consumed by solutions (b) and (a), respectively, for the same pH reading and $(V_L - V_A)$ measures the displacement of the ligand curve with respect to the acid curve. V_0 is the initial volume of the reaction mixture (25 mL), and E^0 and T_L^0 are the resultant concentrations of nitric acid (0.1 M) and HPA (3 mM) in the reaction mixture, respectively. The protonation curves for the proton-ligand system at 15, 25, 35 and 45 °C were obtained by plotting \bar{n}_H vs pH.

\bar{n}_L , the average number of ligands attached per metal ion and pL , the free ligand exponent were determined by the following expressions:

$$\bar{n}_L = \frac{(V_M - V_L)(N + E^0)}{(V_0 + V_A)T_M^0 \bar{n}_H} \quad (2)$$

$$pL = \log_{10} \left[\frac{\sum_{n=0}^{n=j} \beta_n H \left(\frac{1}{\text{anti log pH}} \right)^n}{T_L^0 - \bar{n}_L T_M^0} \times \frac{V_0 + V_M}{V_0} \right] \quad (3)$$

where N , E^0 , V_L , V_0 and V_A have the same meaning as in (1). V_M is the volume of alkali added to solution (c) to attain the pH reading as those of V_A and V_L and T_M^0 is the metal ion concentration (0.6 mM) in the reaction mixture. The metal-ligand formation curves for the Tb(III) complex at various temperatures were obtained by plotting \bar{n}_L vs pL . Proton-ligand formation constant, $\log K_n^{HPA}$ and metal-ligand formation constant, $\log K_n^{Tb}$ were then determined from the protonation curves and metal-ligand formation curves, respectively, by using Bjerrum's half integral method⁵³ as modified by Irving and Rossotti.⁵⁴

Change in free energy (ΔG) was calculated from the formation constant values ($\log K$) at various temperatures using the Gibbs-Helmholtz equation:

$$\Delta G = -2.303RT \log K \quad (4)$$

where R (ideal gas constant) = 8.314 J K⁻¹ mol⁻¹; K = dissociation constant of HPA or stability constant of the complex; T = absolute temperature.

Change in enthalpy (ΔH) for the dissociation of HPA or complex formation was evaluated from the slope of the plots ($\log K_n^{HPA}$ or $\log K_n^{Tb}$ vs $1/T$) using the graphical representation of Van't Hoff's equation (5) and change in entropy (ΔS) could then be calculated using the relationship (6):

$$\Delta G = \Delta H - T\Delta S \quad (5)$$

$$\Delta S = (\Delta H - \Delta G)/T \quad (6)$$

2.4. Synthesis of Tb(III)-HPA Complex

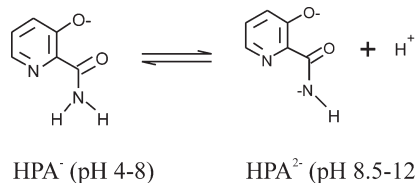
Aqueous solution of TbCl₃·H₂O (0.32 g in 10 mL, 1.0 mmol) was added to an alkaline solution of HPA (1.01 g in 20 mL, 2.0 mmol). The pH of the reaction mixture was adjusted to 7.5 with 0.1 M KOH solution when a light pink precipitate was obtained. The complex was digested on water bath for about 1 hour, suction-filtered and dried in air. Yield: 0.5 g (70 %). IR (ν , cm⁻¹): 3300 (H₂O), 3197, 1541 (NH₂), 1538 (C-O-M), 1648, 1554, 1335 (amide

bands), 475 (Tb-N), 410 (Tb-O); (Found: C, 33.10; H, 2.30; N, 12.73; Tb, 36.52 %. Calc. for $C_{12}H_{10}N_4O_4Tb$ (432.9); C, 33.26; H, 2.31; N, 12.94; Tb, 36.71 %); μ_{eff} : 7.90 BM; Λ_M (10^{-3} M, in DMSO, $\Omega^{-1} \text{ cm}^2 \text{ mol}^{-1}$): 7.80.

3. Results and Discussion

3.1. Protonation and Stability Constants

pH-metric titrations of HPA and Tb(III) complex were performed in aqueous and CTAB micellar media at four different temperatures 15, 25, 35 and 45 °C. The hydroxylpicolinoyl moiety of Virginiamycin S (VS) was shown⁵⁰ to exist in different protolytic forms at pH range 1.2–12.6 (Scheme 1).



Scheme 1

Forms of HPA at different pHs.

At very low pH values ($\text{pH} < 2$), this group was fully protonated while at pH 4.0, the species was present in the zwitterionic form. Increasing pH to about 8.0 would make VS to release one H^+ and on further increase to pH 12, VS released another H^+ from the amine group forming mono- and di-deprotonated species, respectively. In our study, the titration was carried out in the pH range 3.5–10.50 and therefore we expect to observe only the mono-deprotonated form of HPA at $3.5 < \text{pH} < 8.0$. Figure 2 is the representative pH-metric titration curve for Tb(III)-HPA complex in aqueous and CTAB micellar media at 25 °C.

The titration curve of HPA (curve b) shows two inflections at different pHs which may be attributed to the HPA^- and HPA^{2-} forms. However, only the first protonation constant, $\log K_1^{\text{HPA}}$ value corresponding to $\bar{n}_{\text{H}} = 0.5$ could be evaluated from the protonation curves of HPA (Fig. 3) which extend from pH 4.5 to 9.0 thereby showing presence of only one dissociable proton at this pH range. This value is slightly lower than the reported value of 7.84.⁵⁵ Since our experiment starts from pH 4.0, we are not able to obtain another $\log K$ value at $\text{pH} < 3.0$ reported by Anderegg and Raber.⁵⁵

Shift in the buffer region of the ligand to a lower pH upon addi-

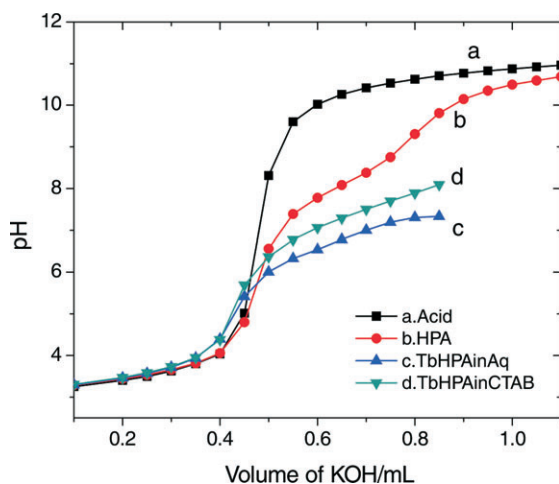


Figure 2 pH-metric titration curves of HPA and Tb(III) complex in aqueous and in CTAB micellar media at 25 °C at ionic strength 0.1 M KNO_3 .

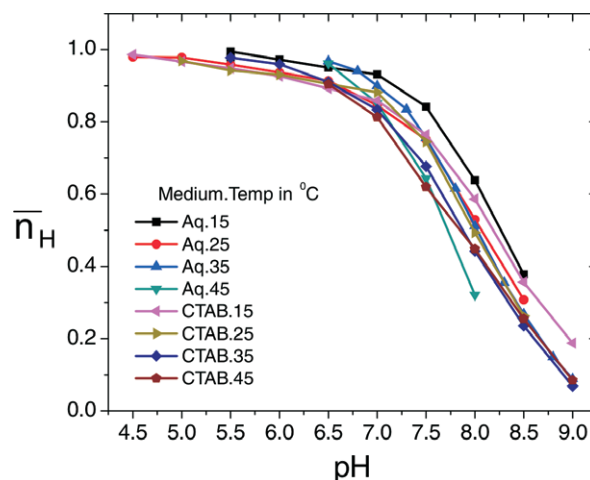


Figure 3 Protonation curves of HPA in aqueous and CTAB micellar media at different temperatures. Maximum value of \bar{n}_{H} (≤ 1.0) shows that HPA exists in the monodeprotonated form.

tion of Tb^{III} to the ligand solution and decrease in pH for the metal titration curves relative to the ligand curve is due to strong metal-ligand interaction. Complex formation competes below pH 8 showing that HPA coordinates to the metal ion only in its uni-negative form. Complex formation curves (Fig. 4) extend to a maximum \bar{n} value 1.8. The values of \bar{n} ($0.20 < \bar{n} < 1.5$) indicate that the complexes formed are of 1:1 and 1:2 metal-ligand stoichiometry.

Protonation constant of the ligand ($\log K_1^{\text{HPA}}$) and stepwise formation constants of the complex ($\log K_1^{\text{Tb}}$ and $\log K_2^{\text{Tb}}$) evaluated from the protonation and complex formation curves at half integrals using Bjerrum's method⁵³ at different temperatures in aqueous and CTAB micellar media are collected in Table 1. Thermodynamic parameters associated with protonation and complexation reactions, i.e. changes in free energy (ΔG), enthalpy (ΔH) and entropy (ΔS) calculated using equations (4), (5) and (6) are also included in Table 1.

It is observed from the table that protonation and complex formation constants of HPA in presence of CTAB are less than those values determined in aqueous media showing that the reactions are more favoured in aqueous medium. Decrease in the stability constant values of Tb(III)-HPA complex with increase in temperature and negative ΔG and ΔH values indicate that the reactions are spontaneous, exothermic and enthalpy-driven in both media.

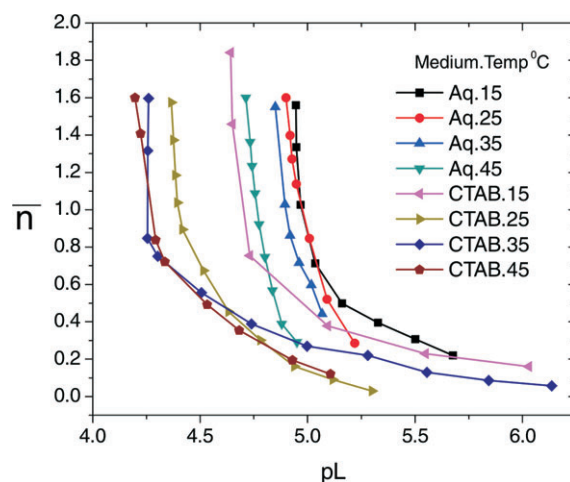


Figure 4 Metal-ligand formation curves of the Tb(III) complex in aqueous and CTAB micellar media at different temperatures.

Table 1 Protonation constants of HPA ($\log K_1^{\text{HPA}}$), stepwise stability constants ($\log K_1^{\text{Tb}}$ and $\log K_2^{\text{Tb}}$) of Tb(III) complex and associated thermodynamic parameters in aqueous and CTAB micellar media at ionic strength 0.1 M KNO_3 .

Medium	Temp/ $^{\circ}\text{C}$	Protonation/Stability constant			Thermodynamic parameters		
		$\log K_1^{\text{HPA}}$	$\log K_1^{\text{Tb}}$	$\log K_2^{\text{Tb}}$	$-\Delta G/\text{kJ mol}^{-1}$	$-\Delta H/\text{kJ mol}^{-1}$	$\Delta S/\text{J deg}^{-1} \text{mol}^{-1}$
Aqueous	15	8.30	5.16	4.95	55.75	30.71	88.62
	25	8.07	5.10	4.91	57.12		
	35	7.95	5.05	4.85	58.38		
	45	7.75	4.85	4.72	58.27		
CTAB	15	8.27	4.98	4.65	53.10	51.16	2.68
	25	8.02	4.61	4.37	51.24		
	35	7.90	4.58	4.26	52.13		
	45	7.85	4.52	4.21	53.15		

The differences between $\log K_1^{\text{Tb}}$ and $\log K_2^{\text{Tb}}$ in Table 1 are all positive and less than unity, which means that the coordination of two ligand molecules to the metal centre occurs almost simultaneously.

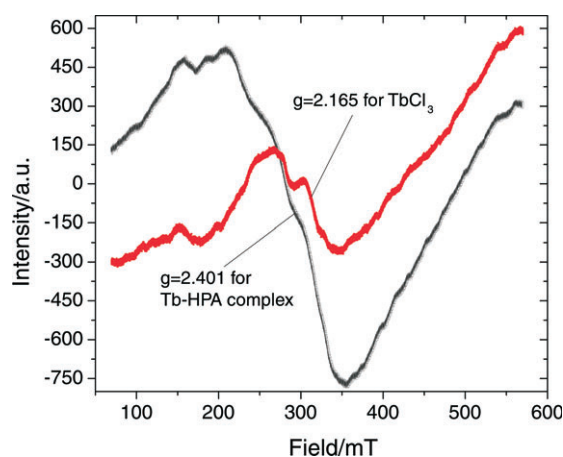
3.2. Characterization of Tb(III)-HPA Complex

The complex is non-melted up to 250 $^{\circ}\text{C}$ and insoluble in water and common organic solvents. Elemental analyses indicate formation of the complex having 1:2 metal:ligand ratio. This corresponds to the pH-metric data. The μ_{eff} value of the complex is lower than the expected value for terbium ion with eight unpaired electrons.⁵⁶ Molar conductance value of the complex at 25 $^{\circ}\text{C}$ in 0.001 M DMSO solution suggests nonelectrolytic behaviour of the complex.⁵⁷ Weight loss observed in the TG/DTA curve of the complex is compatible with presence of two lattice water molecules.

The bonding sites of HPA are assigned based on the comparative analysis of the IR spectra of the ligand shown elsewhere⁴⁷ with that of Tb(III) complex. Shift in the amide bands in the spectrum of Tb(III) complex suggests the coordination of the amido carbonyl oxygen⁵⁸ to Tb^{III} . The sharp band observed at 3393 cm^{-1} in the spectrum of the ligand due to hydroxyl group disappears in the spectrum of the complex with the appearance of a new band at 1538 cm^{-1} assignable to $\nu_{\text{asym}}(\text{COM})$. This probably indicates bonding through the phenolate oxygen.⁵⁹ A broad band around 3300 cm^{-1} indicates presence of water molecules in the complex. Coordination of ring N^{60} may be inferred from the negative shift of the pyridine ring breathing and in-plane vibrations at 1077 and 660 cm^{-1} , respectively, in the spectrum of the HPA to 1053 and 630 cm^{-1} in that of the complex. NH_2 stretching and bending modes show significant changes in the spectrum of the complex thereby suggesting possibility of NH_2 participation in bonding. However, in any of its transition metal complexes,^{45–47} NH_2 group of HPA was not reported to involve in bonding. Participation of the NH_2 group in bonding in the Tb(III) complex may be justified on the ability of the terbium ion to expand its coordination number.

The room temperature ESR spectra of the Tb(III) complex and TbCl_3 are given in Fig. 5 and the spectral features reflect rearrangement of the crystal surroundings of Tb^{III} . The spectrum of the complex consists of one intense and asymmetric line with $g = 2.401$; the asymmetric nature could result from the superposition of more than one resonance line.⁶¹ The asymmetry seems to be higher in the Tb(III)-HPA complex as compared to TbCl_3 ($g = 2.165$) perhaps due to the complexation with HPA.

In the mass spectrum of the complex (Fig. 6), the base peak at m/z 432 with 100 % intensity corresponds to the composition $[\text{Tb}(\text{HPA}-\text{H})_2]$, which is in agreement with the elemental data

**Figure 5** Solid state ESR spectra of Tb(III)-HPA complex and TbCl_3 at room temperature.

and formation of ML_2 species observed in the pH-metric studies. However, appearance of other peaks at higher m/z values suggests formation of species with higher M:L ratio in a polymeric fashion, which perhaps explain the observed lowering in the μ_{eff} value.

Due to the insolubility of the complex, single crystal could not be grown. In absence of a single crystal and after more applicable analysis, a tentative structure for Tb(III) complex showing the bonding sites of HPA and the water molecules satisfying six coordinating sites of Tb^{III} may be proposed as presented in Fig. 7. Coordination of ring-N may occur to other neighboring terbium atom(s).

3.3. Luminescent Studies

Figure 8 shows the emission spectra of TbCl_3 and Tb(III)-HPA complex when excited at 326 nm in aqueous medium. The strong band peaking at 425 nm is associated with the ligand. The characteristic Tb^{III} emission bands originating from the $^5\text{D}_4$ excited state to each of the $^7\text{F}_j$ ($J = 3-6$) ground levels which are very weak in the spectrum of the TbCl_3 are highly sensitized on complexation with HPA. The peaks at 490, 547, 586 and 622 nm are, respectively assigned to the $^5\text{D}_4 \rightarrow ^7\text{F}_6, ^7\text{F}_5, ^7\text{F}_4$ and $^7\text{F}_3$ transitions of Tb^{III} . All the emissions $^5\text{D}_4 \rightarrow ^7\text{F}_j$ ($J = 3-6$) are sensitized by HPA through ligand-to-Tb energy transfer¹⁷ and the sensitization is the most significant for the magnetic dipole transition of Tb^{III} at 547 nm. For such an increase in intensity, energy transfer may not be the only reason. Luminescent quenching may be reduced when the interaction of Tb^{III} with HPA changes its local coordination sphere, accompanied by the substitution of water molecules in the coordination sphere of the metal ion by the ligand, which consequently decreases the luminescent quench-

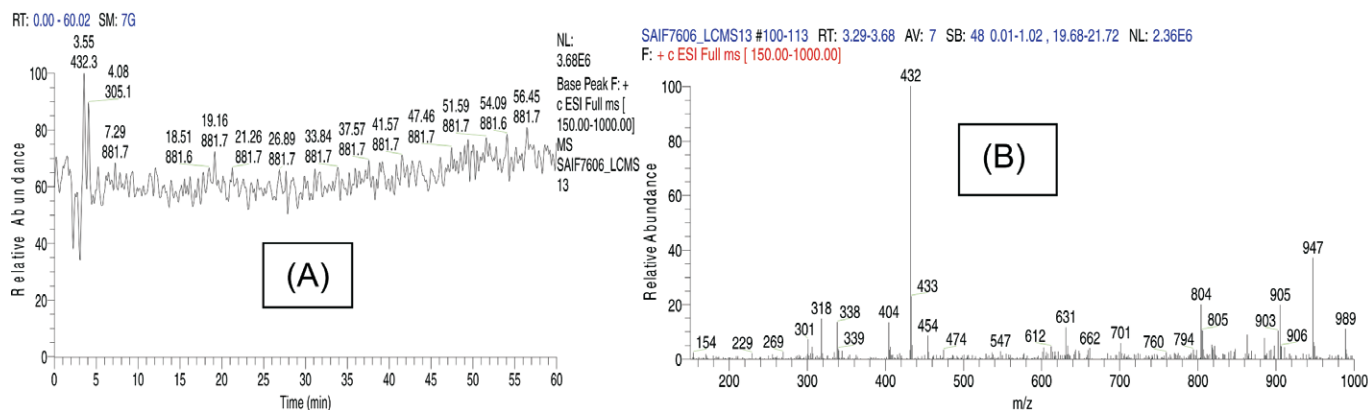


Figure 6 Mass spectrum of Tb(III) complex. (A) Relative abundance of the fragments against time, fragment having molecular mass 432 shows maximum abundance. (B) Base peak at m/z 432 corresponds to $[\text{Tb}(\text{HPA}-\text{H})_2]$ composition. Other peaks at higher m/z values suggest existence of other compositions with higher M:L ratio.

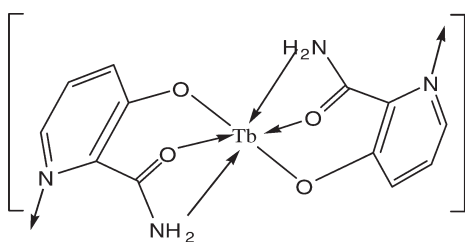


Figure 7 Proposed structure of $[\text{Tb}(\text{HPA}-\text{H})_2] \cdot 2\text{H}_2\text{O}$. IR spectra show bonding through ring-N. Its bonding might have been involved other terbium ion(s) in a polymeric fashion.

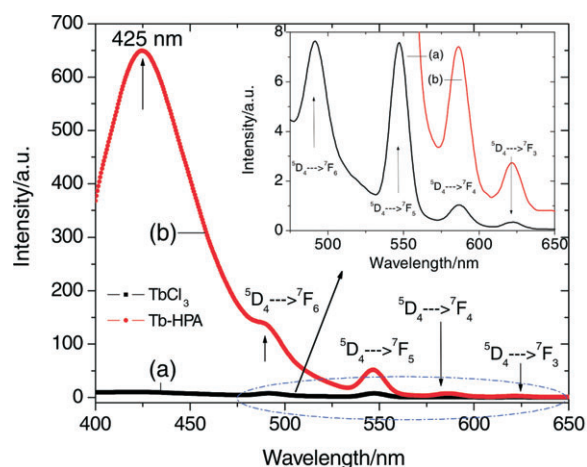


Figure 8 Luminescent spectra ($\lambda_{\text{ex}} = 326$ nm) of (a) TbCl_3 and (b) $\text{Tb}(\text{III})$ -HPA complex in aqueous medium. The inset shows a magnification of terbium emission in the spectral wavelength between 475–650 nm.

ing due to nonradiative depopulation *via* the O-H stretch vibration.^{29,62}

3.3.1. Solvent Effect on Terbium Luminescence

The efficiency of intramolecular energy transfer increases in going from homogeneous solutions to microheterogeneous organized media, such as micellar solutions of surfactants. In many cases, the necessity of a micellar system for the co-luminescent effect was also demonstrated and formation of micelles has apparently a great effect on the increase of the fluorescent intensity in the system.^{63,64} In order to observe the co-luminescent effect of micelles on the luminescent intensity of Tb^{III} , the spectra are recorded in two different sets of solutions containing two surfactants, nonionic Tx-100 and cationic CTAB in their pre-micellar and post-micellar concentrations. The criti-

cal micellar concentrations (CMCs) of Tx-100 and CTAB are 0.24 and 0.92 mM, respectively. Surfactants exist in their monomeric forms in aqueous solutions below their CMCs while they form micelles in aqueous solutions above their CMCs. Comparisons of these spectra have been made with the spectra obtained in aqueous and ethanolic media. Figure 9 exhibits Tb^{III} emission bands in aqueous, ethanol, Tx-100 and CTAB media monitored at the excitation wavelength 326 nm. Significantly enhanced luminescent bands are observed in ethanol and in presence of surfactants as compared to that in aqueous medium. The fluorescent intensity of $\text{Tb}(\text{III})$ is observed to be higher when the concentration of the surfactants are below the respective CMCs of the surfactants and there is a decrease in the intensity of the excitation and emission peaks as the concentration increases above the CMCs. Thus, the effect of the surfactants on the intensity of terbium luminescence is higher in the monomeric forms than in the micellar forms.

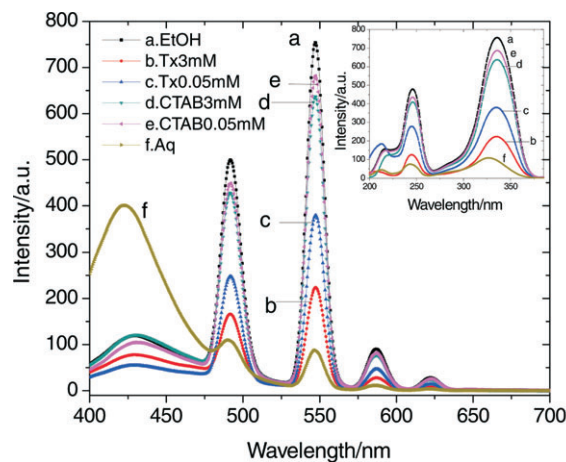


Figure 9 Emission spectra of the complex ($\lambda_{\text{ex}} = 326$ nm) in (a) ethanol, (b) Tx-100 at post-micellar concentration, (c) Tx-100 at pre-micellar concentration, (d) CTAB at post-micellar concentration, (e) CTAB at pre-micellar concentration and (f) in aqueous medium; (Inset, excitation spectra in different media monitored at $\lambda_{\text{em}} = 546$ nm).

The symmetry around the metal ion in the complex can be understood using asymmetric ratio which is defined as the ratio between electric and magnetic dipole transitions as shown by the relationship:

$$A = \frac{\int_{479}^{506} A_1 (\text{electric dipole transition})}{\int_{533}^{561} A_2 (\text{magnetic dipole transition})} \quad (7)$$

where A_1 and A_2 are, respectively, the integrated peak areas of the electric dipole and magnetic dipole transitions of terbium emission bands of Tb(III)-HPA complex. Asymmetric ratio values of the complex in aqueous and in various concentrations of CTAB are collected in Table 2 and the values are found to be less than unity suggesting the occupation of Tb^{III} ions at inversion symmetry site.

A typical fitting Gaussian distribution function to the data of magnetic and electric dipole transitions of Tb(III) complex recorded in different concentration of CTAB is shown in Fig. 10. The optimum concentration of CTAB for highest Tb^{III} luminescence in our study is found to be 0.6 mM as it approaches its CMC (0.92 mM) and this observation agrees with the reported Gd^{III} which shows maximum luminescence in CTMAB at its apparent CMC.⁶⁴

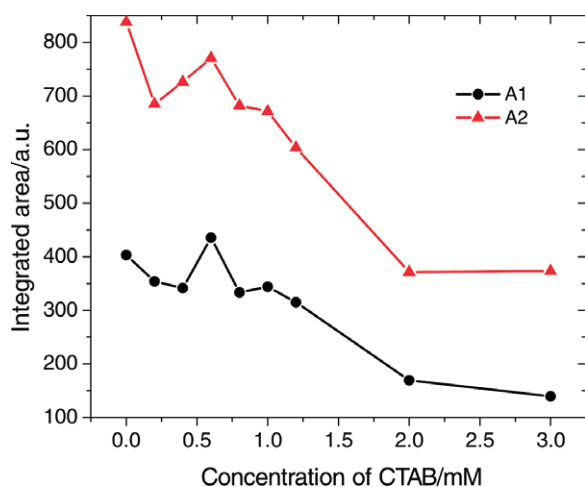


Figure 10 Integrated peak area of the emission bands of Tb(III)-HPA complex (A_1 for $^5D_4 \rightarrow ^7F_6$ and A_2 for $^5D_4 \rightarrow ^7F_5$ transitions) versus concentration of CTAB.

3.3.2. Influence of pH on Terbium Luminescence

pH is an essential parameter of physiological processes which very often operate within a very narrow pH range. Typical examples are enzymes, the activity of which is switched on or off depending on the pH. It is, therefore, natural that many pH sensitive luminescent signalling systems have been developed, some of them based on Ln(III) emission.¹⁰

Figure 11 represents the emission spectra of Tb(III) complex at various pHs and shows that pH has a pronounced effect on both the excitation and emission peaks of terbium. HPA enhances Tb^{III} luminescence the most near neutral pH where the maximum intensity is observed at pH 6.1. Thus, the maximum sensitization

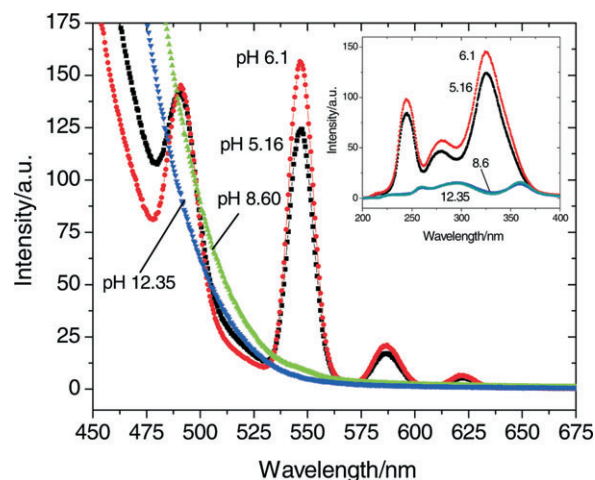


Figure 11 Emission spectra of the complex at different pHs at $\lambda_{ex} = 326$ nm; (Inset, excitation spectra at different pHs monitored at $\lambda_{em} = 546$ nm).

of the Tb^{III} bands is observed at the physiological pH ranges (6.1–7.5) where the complexation occurs. At this pH, deprotonation of HPA results which then binds to Tb^{III} expelling the inner-sphere water molecules. This binding brings the chromophore closer to the lanthanide ion, resulting in a better sensitization of the 4f-centred luminescence.⁶⁵ The luminescent intensity decreases sharply as basicity of the medium increases due to the formation of hydroxylated species $[Tb(OH)_n]^{(3-n)+}$.⁶⁶ At high pHs (>8.0), the characteristic terbium emission bands are not observed except for the strong band of HPA at 425 nm. This clearly suggests that HPA exists in the metal-free form above this pH.

3.3.3. Decay Lifetimes

The luminescent decays of the complex in aqueous and different concentration of CTAB (Fig. 12) were fit very well by biexponential⁶⁷ indicating that the Tb^{III} ions are not distributed homogeneously in the samples. Tb(III) luminescence decay times, τ_1 and τ_2 , for $^5D_4 \rightarrow ^7F_6$ and $^5D_4 \rightarrow ^7F_5$ transitions, respectively, and the average decay times, τ_{av} , are also included in Table 2. The lifetime values are less than those for the heavily quenched Tb(III) aquo systems.^{29,62} Electronic energy transfer among the lanthanide complexes is known to limit the emission intensities of lanthanide activated phosphor systems⁶² and an efficient transfer of energy among Tb(III) complexes would also certainly perturb the emission lifetimes. A random and little difference in decay times with the concentration of the surfactant is observed from the table, which may be rationalized through consider-

Table 2 Integrated peak area of the luminescent spectral bands ($\lambda_{ex} = 326$ nm) for transitions $^5D_4 \rightarrow ^7F_6$ emitted at 490 nm and $^5D_4 \rightarrow ^7F_5$ emitted at 547 nm, asymmetric ratio and decay lifetimes (τ_1 , τ_2 and τ_{av}) of Tb(III) complex in different CTAB concentration keeping $[Tb^{III}]$ constant at 0.20 mM; *aqueous solution of TbCl₃.

CTAB concentration /mM	Integrated peak area		Asymmetric ratio	τ_1 /ms	τ_2 /ms	τ_{av} /ms
	$^5D_4 \rightarrow ^7F_6$ (A_1)	$^5D_4 \rightarrow ^7F_5$ (A_2)				
*Tb ^{III}	0.70	0.97	0.720	0.100	0.369	0.140
0.0	403.48	838.24	0.481	0.060	0.304	0.079
0.2	354.22	684.95	0.517	0.063	0.324	0.075
0.4	341.36	726.02	0.470	0.060	0.300	0.075
0.6	435.37	770.50	0.565	0.057	0.329	0.075
0.8	333.29	682.18	0.489	0.065	0.339	0.076
1.0	343.77	671.21	0.512	0.060	0.299	0.076
1.2	314.90	603.48	0.521	0.063	0.314	0.080
2.0	169.60	371.49	0.457	0.059	0.304	0.077
3.0	139.53	373.12	0.374	0.066	0.322	0.079

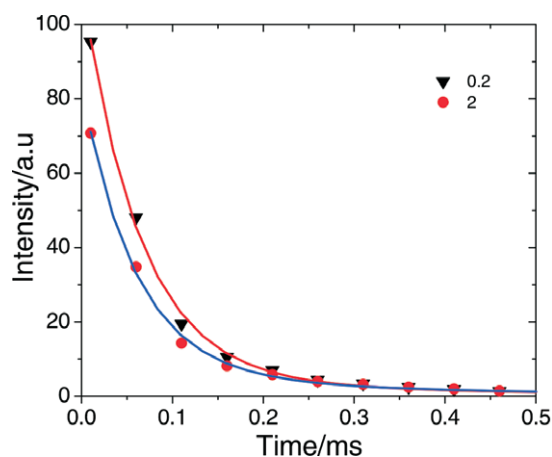


Figure 12 Decay curves monitored around $\lambda_{em} = 546$ nm under $\lambda_{ex} = 326$ nm. The lines represent the data best fits, assuming a biexponential function.

ation of intermolecular energy-transfer properties of the complex in different concentrations of CTAB. It also indicates that the nature of the medium does not exert a significant influence upon the intermolecular energy transfer process and these would only undergo energy-transfer processes through collisional interactions.

4. Conclusions

HPA readily reacts with Tb^{III} in aqueous medium at \sim pH 7.5 to form $Tb(III)$ complex having 1:2 metal-ligand stoichiometry in which HPA binds to Tb^{III} in the deprotonated form. ESR spectrum shows asymmetric arrangement around the metal ion. The luminescence of the HPA-bound $Tb(III)$ complex not only retains the narrow-band, long-lifetime character typical of other $Tb(III)$ chelates in both aqueous and surfactant solutions, but also shows a significant sensitization of the bands on complexation with HPA. The intensity of the magnetic dipole transition of the complex is higher than the electric dipole transition indicating occupation of the Tb^{III} ions at inversion symmetry sites and its insensitiveness to the local symmetry. Though the nature of the medium has minimal effect on the shape and position of the emission bands, pH has a significant effect and the optimum luminescent efficiency is obtained at physiological pH 6–8. Since HPA is used as a model for the study of Virginiamycin S, this study may help in exploring other activities of the antibiotic.

Acknowledgements

The authors acknowledge Sophisticated Analytical Instrumentation Facility, CDRI, Lucknow, for mass spectra and C, H, N analysis data. One of the authors (P.P.) thanks University Grants Commission, New Delhi, for a BSR fellowship.

References

- FS. Richardson, *Chem. Rev.*, 1982, **82**, 541–552.
- I. Hemmilä, *Applications of Fluorescence in Immunoassays*, Wiley Interscience, New York, 1990.
- A.M. Adeyiga, P.M. Harlow, L.M. Vallarino and R.C. Leif, in D.L. Farkas, R.C. Leif, A.V. Priezzhev, T. Askura, B. Tromberg (Eds.), *Progress in Biological Optics*, SPIE Procs. Series, Bellingham, WA, 2678, 1996.
- I. Hemmilä and V. Laitala, *J. Fluoresc.*, 2005, **15**, 529–542.
- J.C.G. Bunzli, *Chem. Rev.*, 2010, **110**, 2729–2755.
- J. Xu, T.M. Corneillie, E.G. Moore, G.-L. Law, N.G. Butlin and K.N. Raymond, *J. Am. Chem. Soc.*, 2011, **133**, 19900–19910.
- S.L.C. Pinho, H. Faneca, C.F.G.C. Geraldés, M.H. Delville, L.D. Carlos and J. Rocha, *Biomaterials*, 2012, **33**, 925–935.
- K. Thorstensen and I. Romslo, *BioMetals*, 1995, **8**, 65–69.
- P. Caravan, J.J. Ellison, T.J. McMurry and R.B. Lauffer, *Chem. Rev.*, 1999, **99**, 2293–2352.
- D. Parker, *Coord. Chem. Rev.*, 2000, **205**, 109–130.
- D. Parker and J.A.G. Williams, in A. Sigel and H. Sigel (Eds.), *Metal Ions in Biological Systems*, Marcel Dekker, New York, 2003, **40**, 233–280.
- D. Parker, *Chem. Soc. Rev.*, 2004, **33**, 156–165.
- D. Parker and Y. Bretonniere, in A.A. Bogdanov Jr. and K. Licha (Eds.), *Molecular Imaging*, 2005, **49**, 123–146.
- S. Pandya, J. Yu and D. Parker, *Dalton Trans.*, 2006, 2757–2766.
- W. C. Floyd, P. J. Klemm, D.E. Smiles, A.C. Kohlgruber, V.R.C. Pierre, J.L. Mynar, J.M.J. Fréchet and K.N. Raymond, *J. Am. Chem. Soc.*, 2011, **133**, 2390–2393.
- A.P. De Silva, H.Q.N. Gunarante, T.E. Rice and S. Stewar, *Chem. Commun.*, 1997, 1891–1892.
- P. K.-L. Fu and C. Turro, *J. Am. Chem. Soc.*, 1999, **121**, 1–7.
- R.M. Supkowski, J.P. Bolender, W.D. Smith, L.E.L. Reynolds and W. DeW. Horrocks Jr., *Coord. Chem. Rev.*, 1999, **185**, 307–319.
- P.H. Brown, A.H. Rathjen, R.D. Graham and D.E. Tribe, in K.A. Gschneider and L. Eyring (Eds.), *Handbook on the Physics and Chemistry of Rare Earths*, North Holland, Amsterdam, Oxford, New York, Tokyo, 1990, **13**, 423–452.
- M. Elbanowski and B. Makowski, *J. Photochem. Photobio. A: Chem.*, 1996, **99**, 85–92.
- C.H. Evans, *Biochemistry of the Lanthanides*, Plenum, New York, 1990, chapter 2–3.
- J.C.G. Bunzli, *Lanthanide Probes in Life, Chemical and Earth Sciences*, Elsevier, Amsterdam, 1989, chapter 7.
- V.W.W. Yam and K.K.W. Lo, *Coord. Chem. Rev.*, 1999, **184**, 157–240.
- C.D.S. Brites, P.P. Lima, N.J.O. Silva, A. Millán, V.S. Amaral, F. Palacio and L.D. Carlos, *New J. Chem.*, 2011, **35**, 1177–1183.
- S. Aime, M. Botta, M. Fasano and E. Terreno, *Chem. Soc. Rev.*, 1998, **27**, 19–29.
- G. Yunusshot and G.W. Mushrush, *Biochemistry*, 1975, **14**, 1677–1681.
- J.C.G. Bunzli and C. Piguet, *Chem. Soc. Rev.*, 2005, **34**, 1048–1077.
- M.N. Hughes, *The Inorganic Chemistry of Biological Processes*, Wiley, New York, 1975.
- J. Reuben, in K.A. Gschneider and L. Eyring (Eds.), *Handbook on the Physics and Chemistry of Rare Earths*, North Holland, Amsterdam, **4**, 1979.
- W. DeW. Horrocks Jr. and D.R. Sudnick, *Acc. Chem. Res.*, 1981, **14**, 384–392.
- R.J.P. Williams, *Struct. Bonding*, 1982, **50**, 79–119.
- Y. Wu, *BioMetals*, 2000, **13**, 195–201.
- S.W. Magennis, S. Parsons and Z. Pikramenou, *Chem. Eur. J.*, 2002, **8**, 5761–5771.
- J.B. Lamture, Z.H. Zhou, A. Sureshkumar and T.G. Wensel, *Inorg. Chem.*, 1995, **34**, 864–869.
- N. Arnaud and J. Georges, *Spectrochim. Acta Part A*, 2003, **59**, 1829–1840.
- P.C.R. Soares-Santos, H.I.S. Nogueira, V. Felix, M.G.B. Drew, R.A. Sa Ferreira, L.D. Carlos and T. Trindade, *Chem. Mater.*, 2003, **15**, 100–108.
- P.C.R. Soares-Santos, F.A. AlmeidaPaz, R.A.S. Ferreira, J. Klinowski, L.D. Carlos, T. Trindade and H.I.S. Nogueira, *Polyhedron*, 2006, **25**, 2471–2482.
- P.C.R. Soares-Santos, L. Cunha-Silva, F.A. AlmeidaPaz, R.A.S. Ferreira, J. Rocha, T. Trindade, L.D. Carlos and H.I.S. Nogueira, *Crystal Growth & Design*, 2008, **8**, 2505–2516.
- P.C.R. Soares-Santos, L. Cunha-Silva, F.A. Almeida Paz, R.A.S. Ferreira, J. Rocha, L.D. Carlos and H.I.S. Nogueira, *Inorg. Chem.*, 2010, **49**, 3428–3440.
- C.M. Granadeiro, R.A.S. Ferreira, P.C.R. Soares-Santos, L.D. Carlos and H.I.S. Nogueira, *J. Alloys and Compounds*, 2008, **451**, 422–425.
- M.E. Mesquita, R.A.S. Ferreira, M. Fernandes, S.C.G. Santos, M.O. Rodrigues, L.D. Carlos and V. de Zea Bermudez, *J. Photochem. Photobio. A Chem.*, 2009, **205**, 156–160.
- M.J.E. Rodrigues, F.A. AlmeidaPaz, R.A.S. Ferreira, L.D. Carlos and H.I.S. Nogueira, *Mater. Sci. Forum (Advanced Materials Forum III)*, 2006, **514-516**, 1305–1312.

- 43 M.O. Rodrigues, J.D.L. Dutra, L.A.O. Nunes, G.F. de Sá, W.M. de Azevedo, P. Silva, F.A.A. Paz, R.O. Freire and S.A. Júnior, *J. Phys. Chem.*, 2012, **C 116**, 19951–19957.
- 44 K.O. Iwu, P.C.R. Soares-Santos, H.I.S. Nogueira, L.D. Carlos and T. Trindade, *J. Phys. Chem.*, 2009, **113**, 7567–7573.
- 45 T.R. Rao and R.K. Lonibala, *Cryst. Res. Technol.*, 1989, **24**, K125–K129.
- 46 K. Sakai, T. Imakubo, M. Ichikawa and Y. Taniguchi, *Dalton Trans.*, 2006, 881–883.
- 47 R.K. Lonibala, Th.P. Devi, Sh. Yumnam and R.K.B. Devi, *Asian J. Chem.*, 2010, **22**, 5389–5398.
- 48 C.M. Granadeiro, S.M.A. Cruz, G. Gonçalves, P.A.A.P. Marques, P.M.F. J. Costa, R.A.S. Ferreira, L.D. Carlos and H.I.S. Nogueira, *RSC Adv.*, 2012, **2**, 9443–9447.
- 49 M.D. Giambattista, G. Ide, Y. Engelborghs and C. Cocito, *J. Biol. Chem.*, 1984, **259**, 6334–6339.
- 50 K. Clays, M.D. Giambattista, A. Persoons and Y. Engelborghs, *Biochemistry*, 1991, **30**, 7271–7276.
- 51 A.I. Busev, V.G. Tipsova, V.M. Ivana, *A Handbook of Analytical Chemistry of Rare Elements*, Ann Arbor-Humphrey Science Publishers, Ann Arbor, London, 1970.
- 52 S.M. Sudhiranjan, N. Homendra and R.K. Lonibala, *Biomaterials*, 2012, **25**, 1235–1246.
- 53 J. Bjerrum, *Metal Ammine Formation in Aqueous Solution*, P. Hasse and Sons, Copenhagen, 1941.
- 54 H.M. Irving and H.S. Rossotti, *J. Chem. Soc.*, 1953, 3397–3405.
- 55 G. Anderegg and M. Raber, *J. Chem. Soc. Chem. Commun.*, 1990, 1194–1196.
- 56 A. Earnshaw, *Introduction to Magnetochemistry*. Academic Press, London, 1968.
- 57 W.J. Geary, *Coord. Chem. Rev.*, 1971, **7**, 81–122.
- 58 B.J. Hathaway, in G. Wilkinson (Ed.), *Comprehensive Coordination Chemistry*, Pergamon, New York, 1987, **5**.
- 59 A. Braibanti, F. Dallavalle, M.A. Pellinghelli and E. Laporati, *Inorg. Chem.*, 1968, **7**, 1430–1433.
- 60 Y. Ionomata, T. Inomata and T. Moriwaki, *Bull. Chem. Soc. Jpn.*, 1974, **47**, 818–824.
- 61 I.N. Botova, A.G. Mirochnik, V.G. Kuryavyi, V.E. Karasev and A.M. Ziatdinov, *Russ. Chem. Bull.*, 1994, **43**, 973–975.
- 62 W. De.W. Horrocks Jr. and D.R. Sudnick, *J. Am. Chem. Soc.*, 1979, **101**, 334–340.
- 63 Y. Xu and I.A. Hemmila, *Anal. Chim. Acta*, 1992, **256**, 9–16.
- 64 C. Tong, Y. Zhub and W. Liua, *Analyst*, 2001, **126**, 1168–1171.
- 65 M.P. Lowe and D. Parker, *Chem. Commun.*, 2000, 707–708.
- 66 C. Bazzicalupi, A. Bencini, A. Bianchi, C. Giorgi, V. Fusi, A. Masotti, B. Valtancoli, A. Rogue and F. Pina, *Chem. Commun.*, 2000, 561–562.
- 67 Z.L. Wang, Z.W. Quan, P.Y. Jia, C.K. Lin, Y. Luo, Y. Chen, J. Fang, W. Zhou, C.J. O'Connor and J. Lin, *Chem. Mater.*, 2006, **18**, 2030–2037.